Jurnal Polimesin
Department of Mechanical Engineering
State Polytechnic of Lhokseumawe
http://e-jurnal.pnl.ac.id/polimesin
e-ISSN : 2549-1999 No. : 6 Month : December
p-ISSN : 1693-5462 Volume : 23 Year : 2025

Processing dates: received on 2025-8-07, reviewed on 2025-10-28, accepted on 2025-11-16 and online availability on 2025-12-31

Experimental evaluation of the thermal and exergy performance of a flat spiral-tube receiver for a parabolic dish collector

Ahmad Yonanda*, Muhammad Raihan Junidy, Muhammad Irsyad, Amrizal, Harmen, Dondi Kurniawan, Angga Darma Prabowo
Department of Mechanical Engineering, University of Lampung, Bandar Lampung 35141, Indonesia
*Corresponding author: ahmad.yonanda@eng.unila.ac.id

Abstract

Global dependence on fossil fuels continues to drive the search for cleaner, more sustainable energy sources. One promising technology is the Parabolic Dish Collector (PDC), harnessing concentrated solar energy. The receiver in a PDC is pivotal to overall thermal efficiency and useful energy output. This study evaluates the thermal and exergy performance of a manufactured flat spiral-tube receiver designed to enhance heat transfer. Experiments were conducted under tropical condition between 10:00 and 14:00 local time at three volumetric flow rates (0.5, 0.8, and 1.1 LPM). The 0.5 LPM flow rate yielded the best performance, with a fluid temperature rise up to 43.8°C, a thermal efficiency of 39.1%, and a peak exergy efficiency of 1.1%. The spiral geometry improved fluid residence time, enabling more effective heat absorption. These findings demonstrate that a simple, manufactured spiral tube receiver can improve PDC performance, offering an efficient and cost-effective solution for solar thermal systems.

Keywords:
Parabolic dish collector, flat spiral-tube receiver, thermal efficiency, exergy analysis, experimental study

1 Introduction

The global energy crisis and escalating greenhouse gas emissions have emerged as significant factors prompting the shift from fossil fuels to cleaner and more sustainable energy sources. Fossil fuels (natural gas, coal, and by-products) are primary contributors to CO_2 emissions, driving environmental damage and long-term climate change (Oludaisi.*et al.*, 2018) [1–3]. Currently, fossil fuels account for over 96% of global energy demand (Muradov, 2017) [4], and are not only finite but take hundreds of millions of years to regenerate. As a result, there is an urgent need to develop effective and sustainable renewable energy technologies.

Among renewable energy sources, solar power stands out as one of the most promising options due to its abundance, near-limitless potential, and environmentally friendly nature [5–9]. Solar energy technologies can generally be categorized into two main types: non-concentrating solar collectors, which operate at low temperatures, and Concentrated Solar Power (CSP) collectors, which operate at much higher temperatures. Among CSP technologies, the Parabolic Dish Collector (PDC) is notable for its high efficiency and capacity to reach peak operating temperatures (Schiel & Keck, 2012) [10].

A crucial element of a PDC system is its receiver, a heat exchanger that captures concentrated solar radiation and transfers the energy to the working fluid. The efficiency of the PDC system is largely influenced by the receiver's material properties, design, and thermal performance. Numerous studies indicate that the shape, material, and internal structure of the receiver play significant roles in determining its heat absorption efficiency. For instance, Loni et al. (2020) showed that a cube-shaped receiver can achieve an efficiency of up to 65.1% [11], while Bellos (2019) reported a 67.95% efficiency for a conical cylindrical receiver at 300°C [12]. Furthermore, research by Soltani et al. (2019) suggests that adjusting the ratio of focal length to aperture diameter in a hollow receiver can enhance thermal efficiency by as much as 65% [13]. Other investigations have also explored the impact of factors such as wind conditions, solar flux distribution, glass layers, and additional fins on improving PDC thermal performance [14–16]. In 2013, Zhang et al. recommended that extending the fluid flow path within the receiver could increase efficiency by allowing more time for heat transfer between the fluid and the heated surface [17]. This theory was validated by Yonanda et al. (2025), whose findings revealed that a mass flow rate of 0.01 kg/s resulted in a higher fluid outlet temperature compared to a flow rate of 0.03 kg/s [18]. This concept has led to the introduction of spiral designs to lengthen the fluid path. Compared to other designs like cavity receivers, conical receivers, or helical receivers, the spiral tube receiver offers simpler manufacturing and enhanced fluid residence time, providing better heat absorption efficiency.

The transition from traditional receiver designs to spiral configurations highlights a significant gap in current research, particularly regarding the optimal balance between simplicity and efficiency. This study aims to fill this gap by investigating the thermal and exergy performance of a spiral flat-pipe receiver in a PDC system, exploring its advantages over more complex receiver types**.** However, many current designs still rely on intricate structures or costly materials, complicating the manufacturing process.

The present study suggests a spiral flat-pipe receiver model as a straightforward yet efficient solution to enhance both thermal and exergy performance in PDC systems. This design not only improves heat transfer efficiency but also reduces manufacturing complexity, making it more affordable [19–21]. Additionally, the research investigates the effect of varying fluid mass flow rates on thermal and exergy performance, offering an initial step towards developing effective, practical, and climate-adaptive PDC technologies suited for tropical environments in Indonesia.

2 Research methodology

This study employs an experimental approach to evaluate the thermal performance and exergy efficiency of a spiral receiver with a flat-pipe design installed in a PDC system. The testing was conducted directly in the field under real conditions, with fluid flow rate as the primary independent variable, varied at 0.5 LPM, 0.8 LPM, and 1.1 LPM. The experiment was conducted in the city of Bandar Lampung, located at approximately 5°20'–5°30' S latitude and 105°28'–105°37' E longitude. Each test was carried out during clear weather conditions between 10:00 AM and 2:00 PM local time (WIB). The tests were carried out over a period of 5 consecutive days, with each experiment conducted at each fluid flow rate tested. This was done to ensure the reproducibility of the experimental result and the stability of the testing conditions. To strengthen the experiment's methodology, the number of days and trials conducted will be specified in subsequent revisions, ensuring reproducibility.

The objective of this experiment is to determine the relationship between fluid flow rate and key performance parameters of the system, including fluid temperature rise, thermal efficiency, exergy efficiency, heat loss, and the Nusselt number.

2.1 Design of the PDC system

The PDC system is designed using a parabolic reflector with a diameter of 1.2 meters, covered by 520 small flat mirrors arranged in a radial configuration. The reflective surface is made of mirror

with a thickness of 2 mm. The focal point of the parabola is located at a distance of 0.529 m from the reflector surface. The complete specifications of the PDC system are presented in Table 1.

Table 1. Specifications of the PDC system

Specification parabolic dish collector	
Parabolic diameter	1.2 m
Parabolic depth (h)	0.3 m
Focal point distance (f)	0.529 m
Reflector surface area	1.134 m^2
Reflector material	Mirror
Mirror thickness	0.002 m
Solar tracking system	Polar-equatorial

The tracking system uses a polar-equatorial method, which allows the dish to follow the sun's movement at a speed of 15° per hour, in accordance with the Earth's rotation.

2.2 Spiral receiver design

In this study, the receiver model adopts a spiral flow path using a flat-tube configuration, designed to provide a more effective flow route and longer fluid residence time to enhance heat transfer performance [22–23]. The receiver features a horizontal spiral flat-pipe design, aimed at increasing the fluid residence time and extending the heat transfer path. Copper was selected as the pipe material due to its high thermal conductivity (398 W/m·K). The complete dimensions of the receiver are presented in Table 2. The spiral receiver is illustrated in Fig. 1.

Table 2. Receiver dimensions

Specification solar receiver	
Receiver diameter	200 mm
Outer pipe diameter	6 mm
Inner pipe diameter	5 mm
Total pipe length	7200 mm
Pipe thickness	0.5 mm
Overall diameter	220 mm
Material (thermal conductivity)	Copper (398 W/m.K)
Surface effectiveness	0.8
Flow geometry	Spiral flat

Fig. 1. Spiral receiver.

The receiver is constructed from a copper pipe with a diameter of 6 mm, manually bent into a spiral shape on a flat plane. The pipe ends are connected at the inlet and outlet points using soldered joints. A metal plate is attached to the base of the receiver, serving both as a support and an additional heat absorber. The entire surface of the receiver is coated with heat-resistant matte black paint to enhance solar radiation absorption and minimize light reflection.

2.3 Experimental setup diagram

In this study, the experimental setup was conducted in an open outdoor environment to ensure sufficient solar radiation and temperature, thereby enabling optimal system performance [24–25] (Fig. 2). The experiment was carried out at three different fluid flow rates: 0.5 LPM, 0.8 LPM, and 1.1 LPM. The testing process begins with a pump that drives fluid from a reservoir to the receiver, passing through a valve and a flow meter. The mass flow rate is controlled by the valve and monitored using the flow meter sensor.

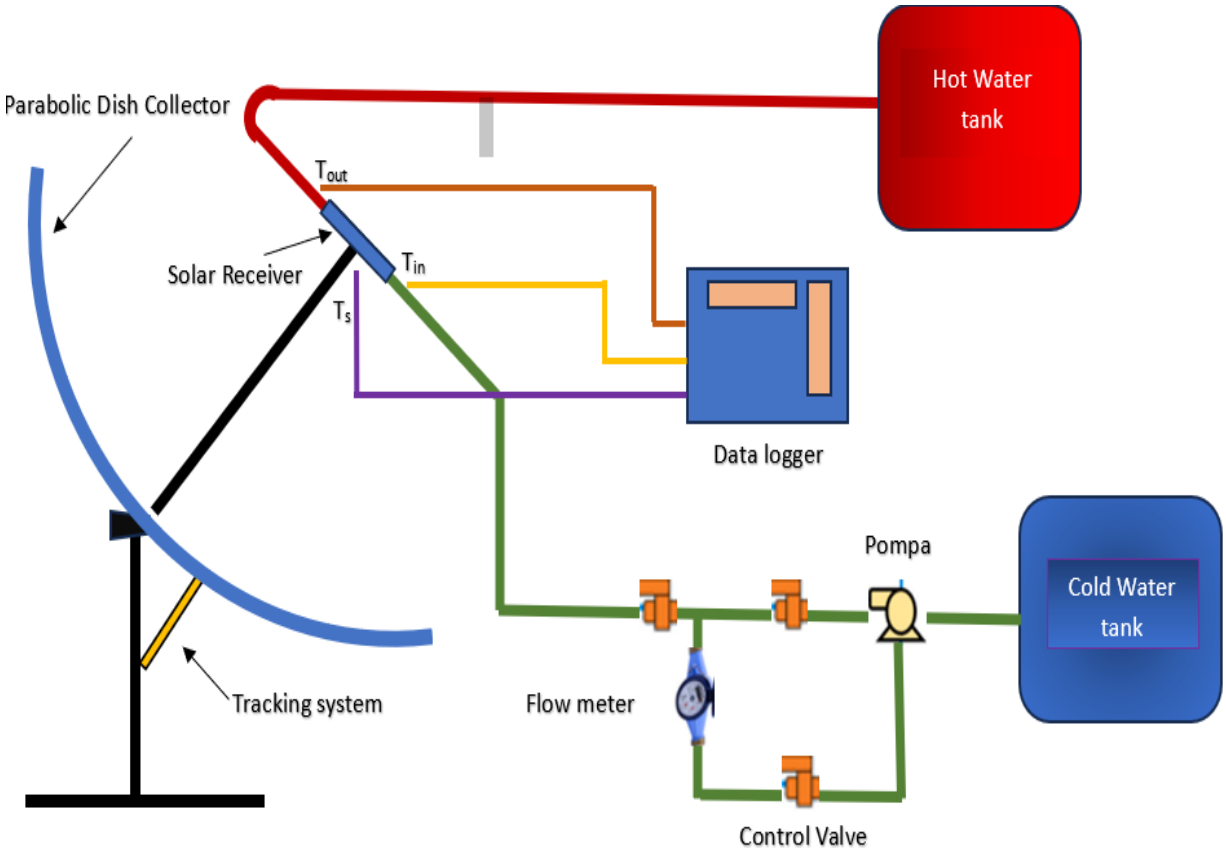

(a)

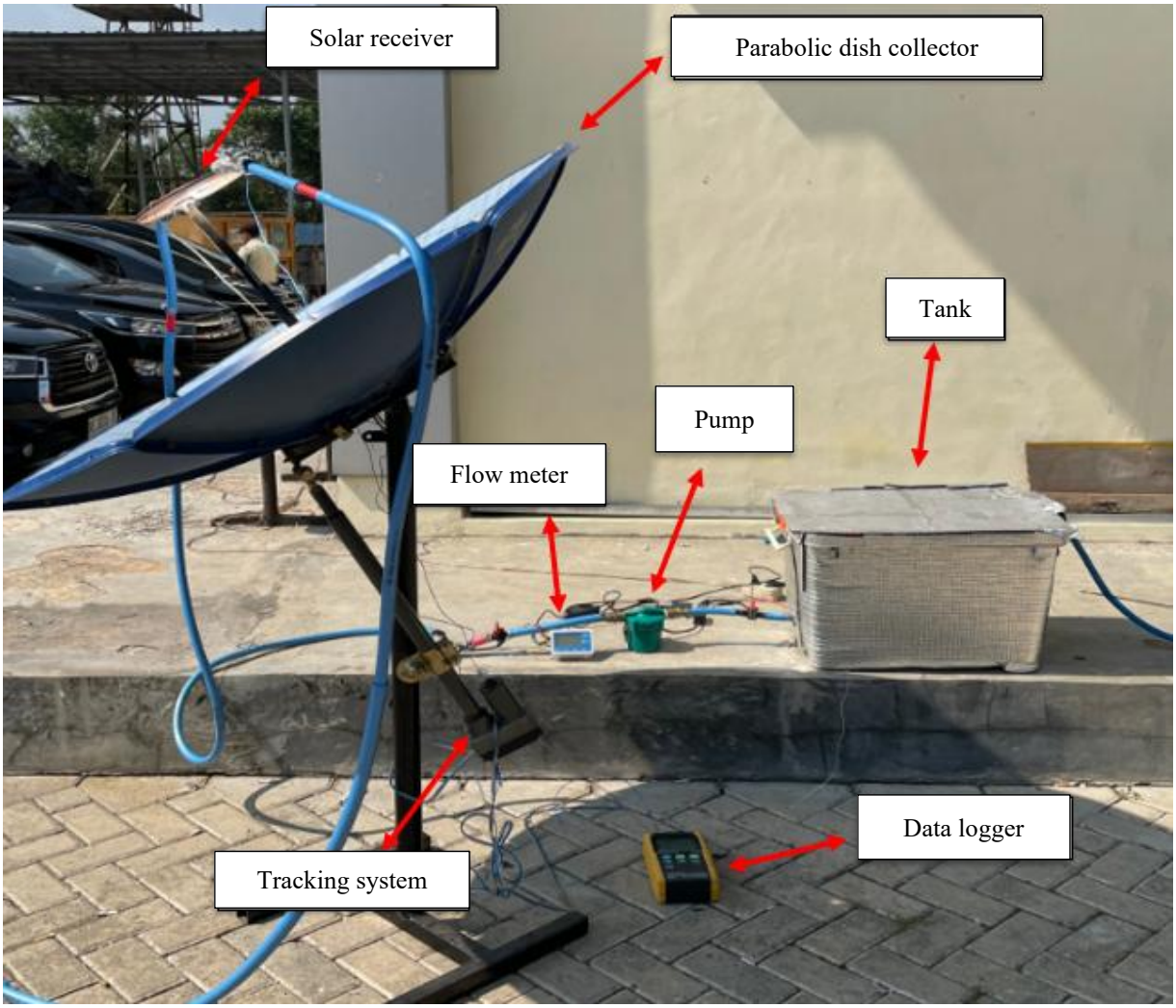

(b)

Fig. 2. (a) Schematic diagram, (b) actual installation photo of the experimental setup.

The aim of this experiment is to establish the relationship between the fluid flow rate and the key performance parameters of the system, including fluid temperature rise, thermal efficiency, exergy efficiency, heat loss, and the Nusselt number. Each parameter is measured using the instruments: (1) fluid temperature rise: measured using a type K thermocouple installed at the fluid inlet and outlet points. The sensor is calibrated using a dry-block calibrator before the tests are conducted to ensure the accuracy of temperature measurements; (2) thermal efficiency: calculated by comparing the energy absorbed by the fluid to the energy received by the system, using a solar power meter to measure the solar radiation incident on the reflector surface; (3) exergy efficiency: calculated using thermodynamic equations based on the energy changes within the system, monitored with pressure and temperature sensors to track the fluid energy variations; (4) heat loss: calculated by measuring the temperature around the receiver using thermocouples and considering the temperature difference between the fluid and the surrounding environment; (5) Nusselt number: determined based on fluid temperature measurements and flow characteristics, using flow meters and thermocouples to calculate the temperature gradient along the receiver surface.

Data from each sensor is collected through a data acquisition system connected to a computer for further processing and analysis (Table 3).

According to the experimental test schematic, Fig. 2(a) illustrates the experimental setup in which water flows from the tank to the solar receiver, driven by a pump that passes through a valve and a flow meter. The tank and pump are positioned at a height of 40 cm to increase the head and reduce the pump's load. The solar receiver is placed at the focal point of the PDC using a support pole, as shown in Fig. 2(b). The PDC system uses the polar-equatorial tracking method, allowing the dish to rotate along an axis parallel to the earth's rotational axis at a constant rate of 15° per hour, matching the earth's rotation speed. The second axis of rotation, the declination axis, is perpendicular to the polar axis.

Table 3. Boundary condition

Parameter	Value
Testing time	10.00 – 14.00 WIB
Location	Bandar Lampung, Indonesia
Ambient temperature	31°C–32°C
Type fluid flow	Water (H_2O)
Inlet water temperature	30°C
Mass flow rates	0.5, 0.02, 0.03 LPM
Receiver geometry	Spiral
Receiver surface emissivity	0.8
Wind speed around	0–5 m/s

2.4 Calculated parameters

To determine the focal point of the parabola in the PDC system, the Eq. (1) as a basic equation [12] is used:

$$f = \frac{d^2}{16h} \tag{1}$$

And to analyze the thermal and exergy performance of the system, the Eq. (2)-Eq. (7) [13] are used. Nomenclature and symbols used in the experiment as shown in Table 4.

1. Heat loss (Q_{loss}):

$$Q_{loss} = Q_{input} - Q_{absorbed} \tag{2}$$

2. Heat loss coefficient (U):

$$U = \frac{Q_{loss}}{A \cdot (T_{receiver} - T_{ambinet})} \quad (3)$$

3. Nusselt number (N_u):

$$N_u = \frac{\left(\frac{f}{8}\right)(Re - 1000)P_r}{1 + 12{,}7\left(\frac{f}{8}\right)^{\frac{1}{2}}\left(P_r^{\frac{2}{3}} - 1\right)} \quad (4)$$

$$f = (0{,}79 \ln R_e - 1{,}64)^{-2} \quad (5)$$

4. Thermal efficiency (η_{th}):

$$\eta_{th} = \frac{\dot{m} \cdot C_p \cdot (T_{out} - T_{in})}{I_b \cdot A} \quad (6)$$

5. Exergy efficiency (η_{ex}):

$$\eta_{ex} = \frac{\dot{m} \cdot C_p \cdot \left[(T_{out} - T_{in}) - T_0 \ln\left(\frac{T_{out}}{T_0}\right)\right]}{I_b \cdot A} \quad (7)$$

Table 4. Nomenclature and symbols used in the experiment

Symbol	Description	Unit
T_{in}	Inlet fluid temperature	°C
T_{out}	Outlet fluid temperature	°C
T_s	Surface temperature of the receiver	°C
I_b	Solar radiation flux	W/m²
$\dot{m}$	Mass flow rate	Kg/s
c_p	Specific heat capacity of water	J/kg.°C
A	Area of the receiver surface	m²
Δt	Time interval for temperature change	s

3 Results and discussion

The experiment was conducted in the city of Bandar Lampung. This location has a tropical climate characterized by high daily solar irradiance. Data collection took place from 10:00 AM to 2:00 PM local time (WIB) on clear days, with ambient temperatures ranging from 31°C to 32°C and maximum wind speeds of up to 5 m/s. These conditions are considered representative for testing the performance of the PDC system under optimal circumstances. This is in line with solar irradiation data from the Meteorological Bulletin of Raden Intan II Station, South Lampung [26], which indicates that the region receives more than 5 hours of sunlight per day on average, with the midday period (approximately 10:00 AM – 2:00 PM) being the peak interval of solar exposure.

3.1 Temperature distribution analysis

Fig. 3 presents the trends in temperature variation and solar radiation intensity (irradiation) at three different fluid flow rates: 0.5 LPM, 0.8 LPM, and 1.1 LPM, over a time range from 10:30 AM to 2:00 PM (WIB). Each graph displays five key parameters: inlet temperature, outlet temperature, ambient temperature, surface temperature, and irradiation value. Flow misdistribution within the heat exchanger system may lead to localized overheating or overcooling, ultimately reducing overall thermal efficiency. According to Chiou [27], tube geometry and the presence of internal obstructions can exacerbate uneven flow distribution, especially at lower flow rates.

Fig. 3(a) flow rate 0.5 LPM (June 7, 2025): at the lowest flow rate, the outlet and surface temperatures increase significantly in response to rising irradiation, peaking between 12:30 PM and 1:00 PM. The surface temperature approaches 50°C, indicating that the fluid has a longer residence time within the system, allowing for higher heat absorption. This demonstrates high energy absorption efficiency at low flow rates, albeit with the risk of potential overheating. These results align with Zhang *et al.* (2013), who noted that increased fluid contact time with the heated surface positively influences temperature rise.

Fig. 3(b) flow rate 0.8 LPM (June 22, 2025): when the flow rate is increased to 0.8 LPM, the temperature rise pattern becomes more moderate. Outlet and surface temperatures still increase, but within a more controlled range. The peak irradiation occurs around 12:00 PM, followed by a stabilization in temperature. This indicates that a medium flow rate can provide balance between heat absorption efficiency and thermal stability, making it an optimal condition for continuous operation.

Fig. 3(c) flow rate 1.1 LPM (June 26, 2025): at the highest flow rate, the temperature response to irradiation fluctuations becomes slower and less pronounced. Despite irradiation exceeding 1100 W/m², the outlet and surface temperatures show only slight increases. This indicates that higher flow rates reduce the fluid's contact time with the heated surface, leading to lower heat absorption. However, this also demonstrates the system's advantage in avoiding excessive heat accumulation, thereby reducing thermal stress on the materials.

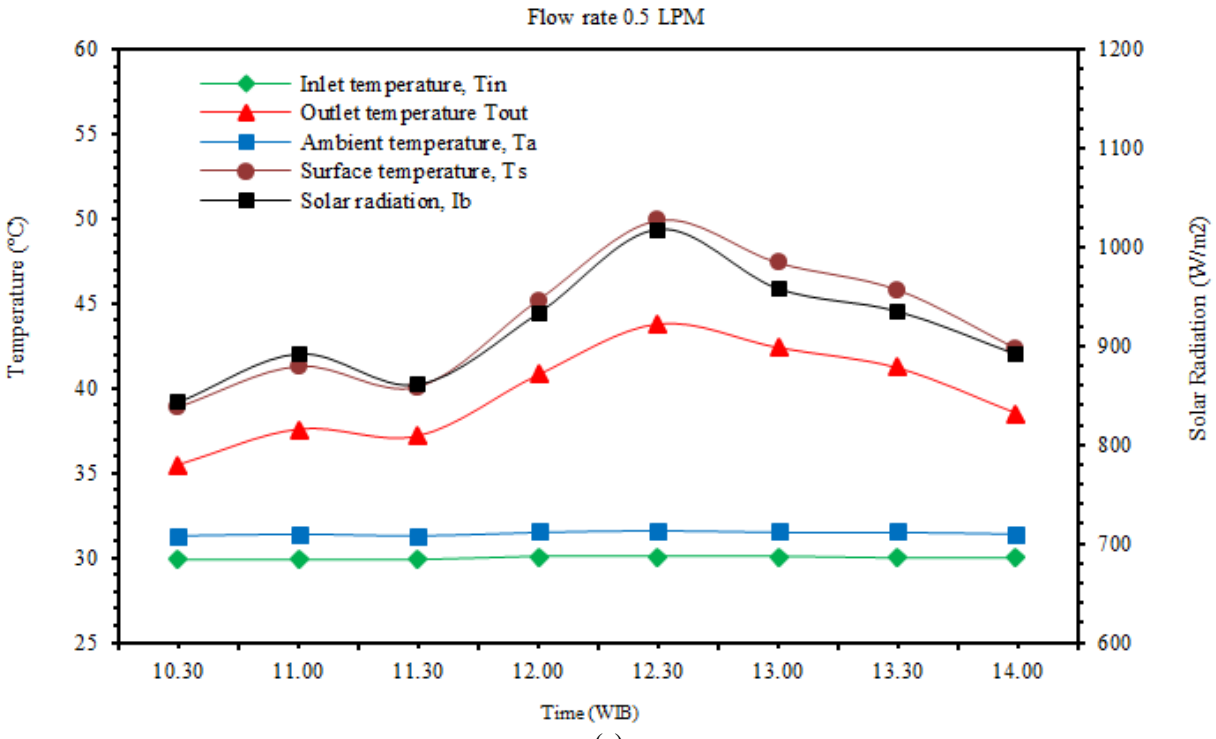

(a)

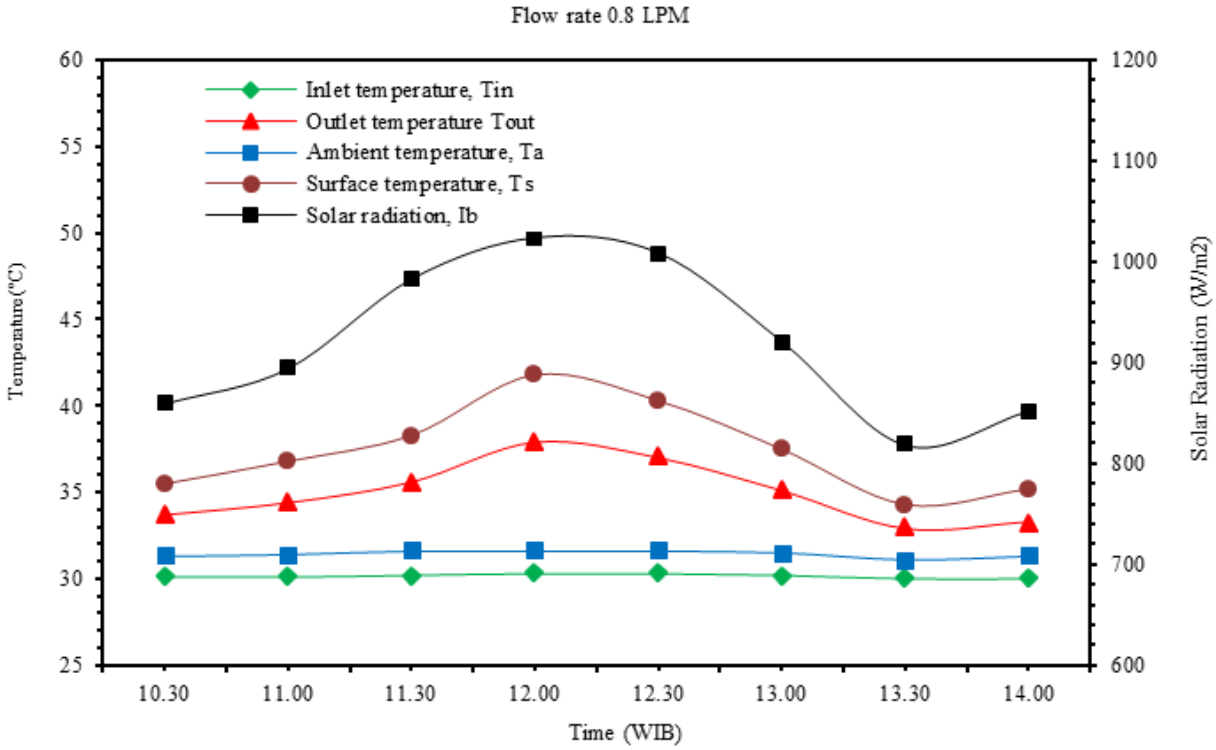

(b)

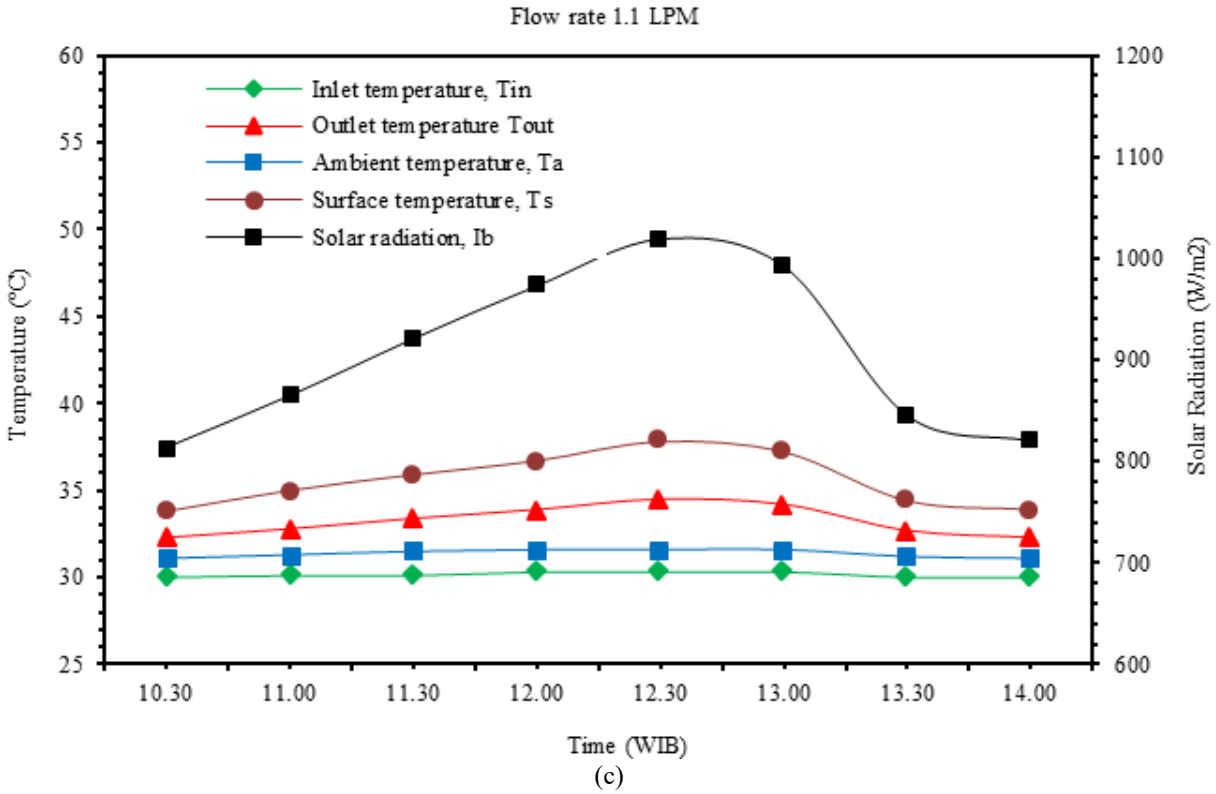

(c)

Fig. 3. Temperature and solar radiation distribution over time at different fluid flow rates: (a) 0.5 LPM, (b) 0.8 LPM, and (c) 1.1 LPM.

This study adopts an experimental approach to compare the thermal performance of a spiral flow tube receiver at three different flow rates. Its novelty lies in the real-time simultaneous monitoring of outlet temperature, surface temperature, and solar irradiation—an aspect rarely examined in spiral-type parabolic collector systems. The 30-minute interval observations also enable more precise thermal analysis of microclimate dynamics.

3.2 Heat loss evaluation

Subsequently, an analysis of heat loss in the receiver was conducted to optimize the receiver design. Heat loss refers to the amount of thermal energy lost from the solar receiver system, including losses due to convection and radiation. Calculating this parameter is crucial for evaluating the thermal performance of the solar receiver, as it plays a significant role in optimizing both the design and operation of the receiver system. The data on heat loss in the receiver are presented in Fig. 4.

Fig. 4 presents the temporal variation of heat loss and solar radiation between 10.30 and 14.00 for three different mass flows. The heat loss show this figure was calculated from the energy balance in Eq. (2). The overall pattern reflects typical tropical midday behavior, where both parameters gradually increase from late morning. Reach their peak around 12.30, and subsequently decrease as solar radiation declines. This trend is not only visually observable but is also supported by quantitative data.

For the 0.5 LPM mass flow rate, heat loss rises from 200 W at 10:30 to 470 W at 12:30, before dropping to 300 W at 14:00. During the same period, solar irradiance increases from 360 W/m²

at 10:30 to a peak of 420 W/m² at 12:30, then decreases to 370 W/m² by 14:00. When these heat-loss and irradiance data points are statistically examined across all time intervals, a strong linear association is found. Pearson's correlation coefficient yields r = 0.95, confirming that the rise in solar irradiance significantly contributes to the increase in heat loss on the receiver surface. This suggests that the lower fluid flow enhances convective heat transfer within the spiral tube but also results in greater heat release to the environment due to a larger temperature gradient between the pipe surface and the surrounding air.

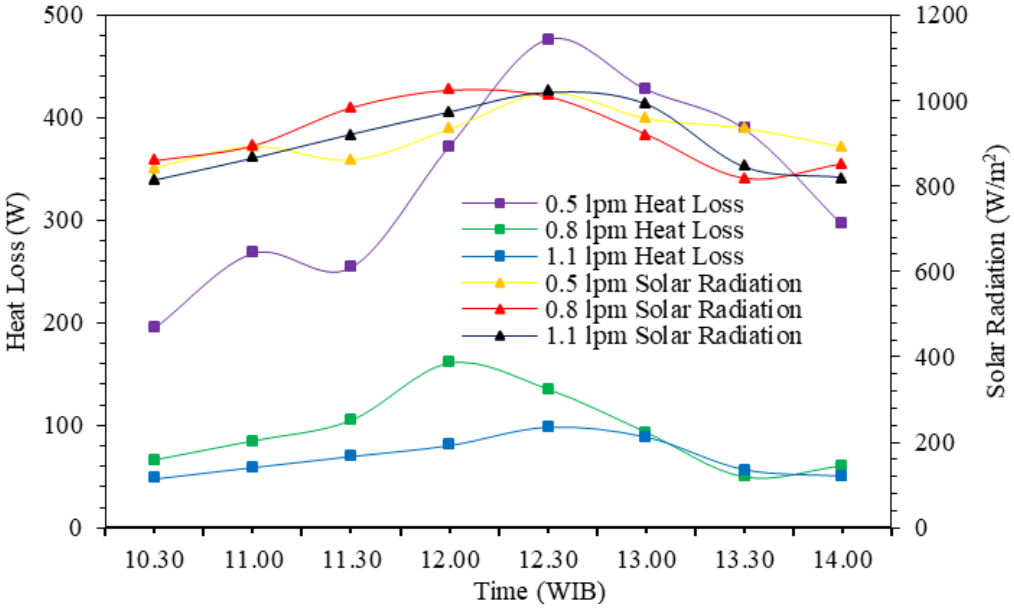

Fig. 4. Heat loss graph based on mass flow rate variation.

Similar tendencies are observed at 0.8 LPM and 1.1 LPM, although with different magnitudes of heat loss. At 0.8 LPM, maximum heat loss is approximately 165–170 W, whereas at 1.1 LPM, it is in the range of 95–100 W. These quantitative differences indicate that higher flow rates reduce the wall-surface temperature, decreasing the temperature gradient with ambient air and therefore lowering convective heat loss. Faster-moving fluid absorbs heat more rapidly, retaining more thermal energy within the fluid rather than releasing it into the environment.

In terms of solar radiation, the observed pattern follows a typical tropical midday trend—intensity rises until it reaches a maximum around 12:30 PM, and then gradually declines. The peak solar irradiance recorded was approximately 1000 W/m². This trend is consistent across all flow rate variations, indicating that solar radiation levels are more strongly influenced by external factors such as sun position and atmospheric conditions than by the characteristics of the fluid system itself.

A noticeable relationship is observed between heat loss and solar radiation at the peak values of each curve. As the intensity of radiation increases, so does the heat loss, particularly at higher flow rates. This indicates that some of the absorbed solar energy is not entirely transferred to the working fluid, but instead dissipates into the surroundings through conduction and natural convection. Heat dissipation occurs primarily through convention and radiation, with factors such as temperature gradients, wind speed, and material properties influencing the heat loss. Convection is more pronounced at lower flow rates due to the larger temperature gradient between the pipe surface and ambient air, while radiation increases with surface temperature. To improve system performance, strategies aimed at minimizing heat loss, such as using insulating materials or selective absorption coatings, are critical. Kim *et al.* [28] have proposed a simplified model for heat loss, incorporating both conduction and free convection, while Nguyen *et al.* [29] have investigated the impact of water-cooling rates on the performance of solar collectors. However, the applicability of these models to the spiral tube receiver system in our study requires adaptation. The specific geometry of the spiral tube, combined with its unique fluid dynamics, means that these models must be modified to account for the flow characteristics and heat transfer efficiencies inherent in spiral tube designs. Future studies could focus on validating these models for spiral receivers by comparing their predictions with experimental data specific to our system, allowing for more accurate predictions of heat loss in such designs.

These findings carry significant implications for the design of solar collector systems. Flow rates that are too high (such as 1.1 LPM) may result in inadequate heat absorption, despite their role in reducing heat loss—especially during periods of peak solar radiation. Therefore, finding an optimal flow rate is crucial to strike a balance between maximizing heat absorption efficiency and minimizing heat loss. The results underline the necessity of selecting the right operational parameters for spiral flow tube receiver systems.

The real-time observation method employed in this study allows for a precise identification of fluctuations in thermal performance over short intervals. By integrating data on irradiance, outlet temperature, and heat loss, the study provides a comprehensive understanding of the system's thermal behavior under various environmental and operational conditions.

3.3 Convective heat transfer and Nusselt number analysis

The Nusselt number (Nu) is a dimensionless quantity used in heat transfer studies to represent the ratio of convective to conductive heat transfer within a fluid. This value is closely related to the convective heat transfer coefficient, as they are directly proportional. A higher Nusselt number indicates a greater convective heat transfer coefficient, reflecting improved efficiency of the convective heat transfer process. The convective heat transfer coefficient and the Nusselt number are determined based on the Reynolds number and Prandtl number using the Gnielinski correlation equation [30].

Fig. 5 presents the convective heat transfer coefficient (h) and the Nusselt number (N_u) over time, for three different fluid flow rates: 0.5 LPM, 0.8 LPM, and 1.1 LPM. The values of h and N_u plotted in this figure were obtained by substituting the instantaneous values of R_e and P_r into Gnielinski correlation in Eq. (4) and subsequently into Eq. (5) for each flow rate condition. These two parameters are used to evaluate the ability of the spiral flow tube receiver system to transfer heat from the pipe wall to the working fluid during the heating process. In general, it can be observed that the higher the flow rate, the greater the values of both the convective heat transfer coefficient and the Nusselt number

tend to be. This can be explained by the basic nature of convection: when the fluid flows faster, the thermal boundary layer becomes thinner, resulting in more efficient heat transfer between the pipe wall and the fluid. This is clearly seen at the 1.1 LPM flow rate, where h reaches over 1300 W/m²·K and Nu is around 11.5, significantly higher than the 0.5 LPM flow rate which only reaches around 800 W/m²·K and N_u close to 7.5. Similar trends have been report in the literature for instance; Loni *et al*. [11] observed that increasing flow rate in a solar tubular receiver led to increased N_u and h.

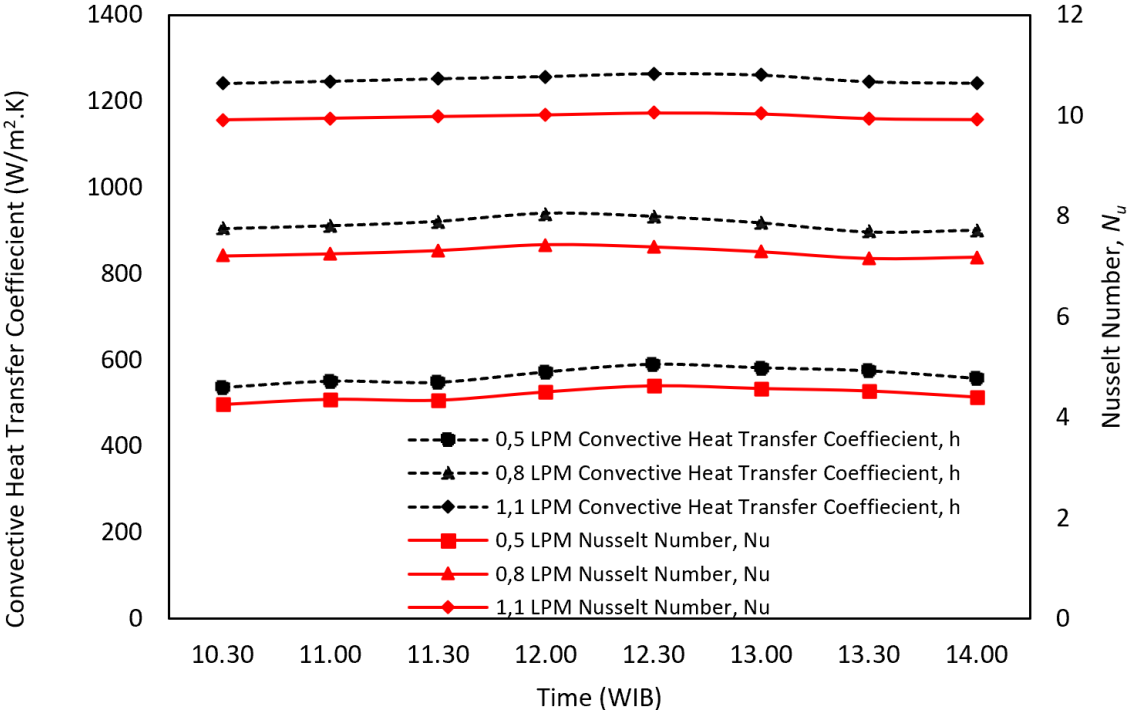

Fig. 5. Graph of convective heat transfer coefficient and Nusselt number at 1.1 LPM.

In addition to comparing flow rates, the graph also shows that both h and N_u values remain relatively stable over time, with only slight fluctuations around midday. This indicates that the heat transfer performance of the system is quite consistent despite variations in solar radiation, which can be assumed to be evenly absorbed by the spiral tube surface. This stability suggests that the spiral receiver design is effective in maintaining thermal performance under changing environmental conditions. The Nusselt number in this context represents forced convection, and its value strongly correlates with the Reynolds number (which increases with higher flow rates). A higher N_u indicates that the dominant heat transfer mechanism is internal convection, rather than mere surface conduction. These findings reinforce the conclusion that increasing the fluid flow rate contributes positively to convective heat transfer efficiency. However, increasing the flow rate should also be considered from the standpoint of pump energy requirements and the potential increase in mechanical losses, making flow rate optimization an essential aspect in system design. This tradeoff between enhanced heat transfer and increase pumping power is also widely discussed in heat exchanger literature [20].

3.4 Comparison of thermal and exergy efficiencies

This study also examines thermal efficiency and exergy efficiency as two key parameters in analyzing the performance of a solar receiver. These two parameters are interrelated but assess different aspects of energy utilization. Thermal efficiency represents the system's ability to convert the received solar thermal energy into the thermal energy of the working fluid and is evaluated in this work using the energy balance formulation given in Eq. (2). Meanwhile, exergy efficiency provides an overview of how effectively this energy is utilized to produce useful work, taking into account thermodynamic limitations and irreversibility losses in the process [31]. Analyzing both efficiencies is essential to gain a comprehensive understanding of the system's thermal performance and energy optimization potential in a holistic manner. The value of thermal efficiency and exergy efficiency discussed in this section were obtained at each time step by substituting the measured solar radiation, mass flow rate, and inlet-outlet temperatures into Eq. (6) and Eq. (7) for the different flow rate conditions.

Fig. 6 illustrates the variations in thermal efficiency and exergy efficiency of the spiral flow tube receiver system over time for each fluid flow rate: 0.5 LPM, 0.8 LPM, and 1.1 LPM. These two parameters are essential in evaluating the performance of a thermal system not only from the perspective of the amount of energy absorbed, but also in terms of the quality and thermodynamic usefulness of that energy.

At a flow rate of 0.5 LPM (Fig. 6(a)), thermal efficiency exhibits a steady increase from morning hours, peaking around 12:34 PM (WIB) at nearly 60%. At the same time, energy efficiency also rises sharply and reaches a maximum value of about 1.1%. This indicates that a portion of the absorbed energy is not only retained in the working fluid but is also available to perform useful work. From an exergy standpoint, an efficiency of 1.1% at 0.5 LPM can be classified as moderate and falls within the range typically reported for small-scale solar thermal systems in the literature, indicating that the present receiver operates at a realistic level of thermodynamic performance and can serve as a reasonable baseline for further design optimization. Under these low-flow conditions, the transferred thermal energy therefore has a relatively high thermodynamic quality, although conductive and convective heat losses from the receiver surface may increase. Such magnitudes of exergy efficiency are consistent with the findings of Chand *et al*. [9] and Schiel *et al*. [10], who reported that small-scale solar thermal collectors typically achieve exergy efficiencies between 1% and 3% under low-flow conditions.

In contrast, at a flow rate of 0.8 LPM (Fig. 6(b)), both thermal and exergy efficiencies show a sharp surge toward midday, peaking at approximately 50% for thermal efficiency and 0.45 for exergy efficiency. However, after reaching its peak, exergy efficiency experiences a significant decline, dropping close to zero by late afternoon. This decline indicates that although energy absorption remains significant (as thermal efficiency stays relatively high), the quality of that energy decreases due to increased system entropy, caused by high temperature gradients between the fluid and the surrounding environment. Such behavior has also been documented

in studies of parabolic trough and compound receiver systems under fluctuating solar irradiation [14], further supporting the present result.

At the highest flow rate of 1.1 LPM (Fig. 6(c)), an interesting phenomenon occurs. Thermal efficiency continues its upward trend toward midday and remains above 40%, yet exergy efficiency is significantly lower, with a peak value of only about 0.11—much lower than the values observed at the other two flow rates. This indicates that although energy transfer into the system is efficient, the high fluid velocity results in a shorter heat contact time, preventing optimal thermodynamic conversion into useful work. Consequently, a portion of the energy is retained as latent heat, which is not fully utilized.

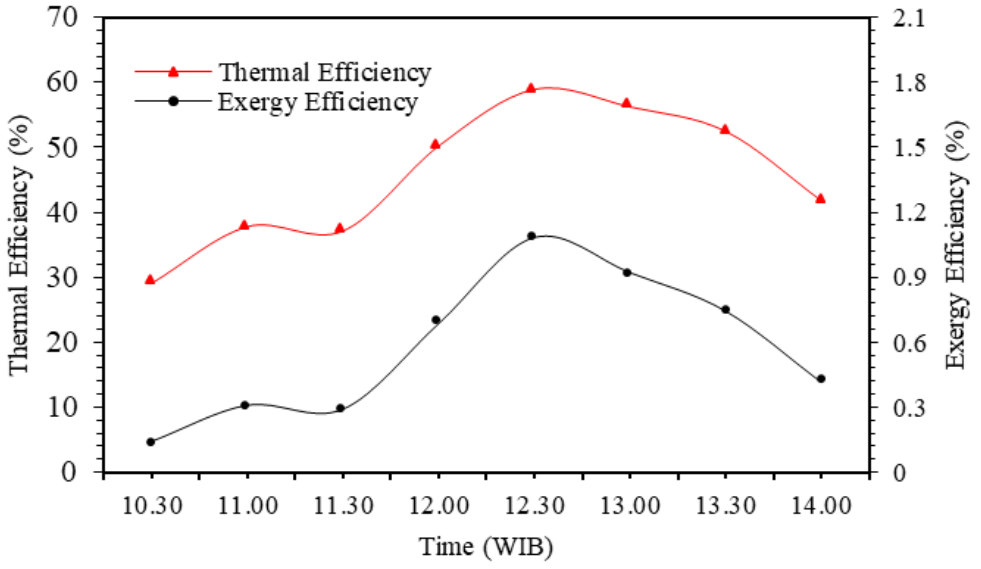

(a)

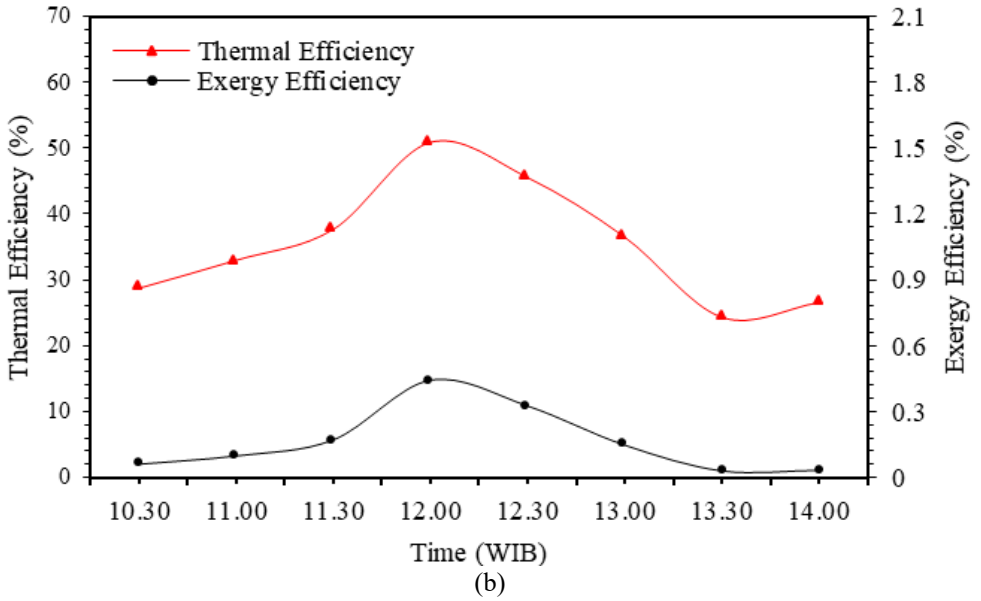

(b)

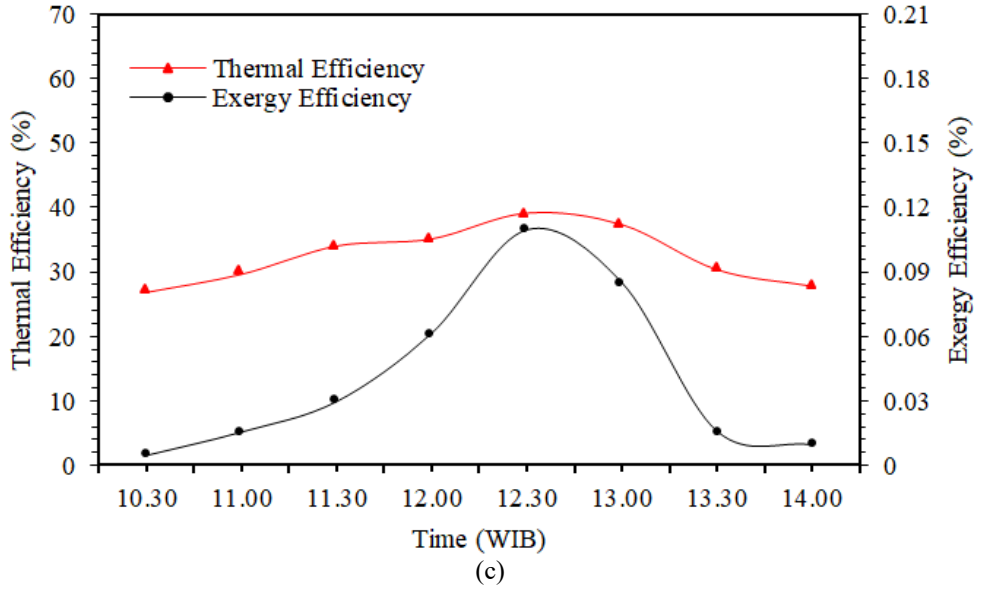

(c)

Fig. 6. Graphs of thermal efficiency and exergy efficiency over time at flow rates of (a) 0.5 LPM, (b) 0.8 LPM, and (c) 1.1 LPM.

A comparison of the three graphs reveals that thermal efficiency does not always correlate directly with exergy efficiency. Higher flow rates may reduce heat losses but simultaneously lower the quality of the resulting energy. Conversely, lower flow rates allow the fluid to absorb heat more uniformly, producing energy that is more thermodynamically "ordered." This decoupling between energy and exergy performance has been emphasised by multiple researchers, including Chiou [27] and Nguyen *et al.* [29], who argued that the optimal operating point of any solar thermal system must consider not only energy efficiency but also exergy efficiency as a determinant of the real usefulness of the delivered heat**.** Therefore, achieving a balance between energy quantity and quality requires selecting an optimal flow rate—one that considers both thermal efficiency and exergy efficiency as key indicators of practical system performance.

4 Conclusions

The experimental results show that variations in fluid flow rate significantly influence system performance: at 0.5 LPM, the maximum thermal efficiency reaches about 60% and the exergy efficiency about 1.1%, while at 0.8 LPM these values are approximately 50% and 0.45, and at 1.1 LPM around 40% and 0.11, respectively. Although the highest exergy efficiency is obtained at 0.5 LPM due to longer heat contact time, the highest convective heat transfer coefficient and Nusselt number are observed at 1.1 LPM (up to ~1300 W/m²·K and Nu ≈ 11.5), indicating more intense convective heat transfer but a reduction in the thermodynamic quality of the useful energy. These results suggest that a moderate flow rate, such as 0.8 LPM, offers a practical compromise between minimizing heat loss, maintaining acceptable thermal efficiency, and preserving a reasonable level of exergy efficiency, which is relevant for the design and operation of small-scale parabolic dish systems in real tropical applications. The simultaneous monitoring of outlet temperature, receiver surface temperature, and solar irradiance in real time has enabled a more detailed assessment of the receiver response to microclimatic variations.

References

[1] A. OLUDAISI, A. KAYODE, AND O. AYODEJI, "Bridging Environmental Impact Of Fossil Fuel Energy: The Contributing Role Of Alternative Energy," *Journal of Engineering Studies and Research*, vol. 23, no. 2, Apr. 2018, DOI: 10.29081/jesr.v23i2.267.

[2] Z. L. Lu, L. L. Wang, X. P. Guo, J. Pang, and J. J. Huan, 'Decoupling effect and influencing factors of carbon emissions in China: Based on production, consumption, and income responsibilities', Advances in Climate Change Research, 2024, doi: 10.1016/j.accre.2024.10.001.

[3] H. Niu, S. Chen, and D. Xiao, 'Multi-Scenario land cover changes and carbon emissions prediction for peak carbon emissions in the Yellow River Basin, China', Ecol Indic, vol. 168, Nov. 2024, doi: 10.1016/j.ecolind.2024.112794.

[4] N. Muradov, "Low To Near-Zero Co2 Production Of Hydrogen From Fossil Fuels: Status And Perspectives," May 18, 2017, *Elsevier Ltd*. DOI: 10.1016/j.ijhydene.2017.04.101.

[5] D. Barlev, R. Vidu, and P. Stroeve, "Innovation In Concentrated Solar Power," 2011, *Elsevier B.V.* DOI: 10.1016/j.solmat.2011.05.020.

[6] A. Aacharya, H. Davidsson, B. Baral, and M. Andersson, 'Investigation of thermodynamics performance of a heat exchanger-incorporated solar dryer equipped with double-pass flat, v-corrugated, and low-e coated collectors for drying applications', Case Studies in Thermal Engineering, vol. 64, Dec. 2024, doi: 10.1016/j.csite.2024.105482.

[7] A. Kumar, B. K. Sharma, T. Muhammad, and L. M. Pérez, 'Optimization of thermal performance in hybrid nanofluids for parabolic trough solar collectors using Adams–Bashforth–Moulton method', Ain Shams Engineering Journal, 2024, doi: 10.1016/j.asej.2024.103106.

[8] S. Theeyzen and B. Freegah, 'The effect of added wire mesh on the thermal efficiency of the flat plate solar water heater collector', Results in Engineering, vol. 24, Dec. 2024, doi: 10.1016/j.rineng.2024.103203.

[9] S. Chand, A. Kumar, M. Srivastava, A. Kumar, J. Giri, and A. Fatehmulla, 'Impact of collector aspect ratio on the energy and exergy efficiency of a louvered fin solar air heater', Case Studies in Thermal Engineering, vol. 63, Nov. 2024, doi: 10.1016/j.csite.2024.105312.

[10] W. Schiel and T. Keck, "Parabolic Dish Concentrating Solar Power (Csp) Systems," In *Concentrating Solar Power Technology*, Elsevier, 2012, pp. 284–322. DOI: 10.1533/9780857096173.2.284.

[11] R. Loni *et al.*, "Research And Review Study Of Solar Dish Concentrators With Different Nanofluids And Different Shapes Of Cavity Receiver: Experimental Tests," *Renew Energy*, vol. 145, pp. 783–804, Jan. 2020, DOI: 10.1016/j.renene.2019.06.056.

[12] E. Bellos, "Progress In The Design And The Applications Of Linear Fresnel Reflectors – A Critical Review," May 01, 2019, *Elsevier Ltd*. DOI: 10.1016/j.tsep.2019.01.014.

[13] S. Soltani, M. Bonyadi, and V. Madadi Avargani, "A Novel Optical-Thermal Modeling Of A Parabolic Dish Collector With A Helically Baffled Cylindrical Cavity Receiver," *Energy*, vol. 168, pp. 88–98, Feb. 2019, DOI: 10.1016/j.energy.2018.11.097.

[14] V. Madadi Avargani, A. Rahimi, M. Divband, and M. A. Zamani, "Optical Analysis And Heat Transfer Modeling Of A Helically Baffled Cavity Receiver Under Solar Flux Non-Uniformity And Windy Conditions," *Thermal Science And Engineering Progress*, vol. 20, Dec. 2020, DOI: 10.1016/j.tsep.2020.100719.

[15] S. Eterafi, S. Gorjian, and M. Amidpour, "Effect of Covering Aperture of Conical Cavity Receiver on Thermal Performance of Parabolic Dish Collector: Experimental and Numerical Investigations," *Journal of Renewable Energy and Environment*, vol. 8, no. 4, pp. 29–41, Oct. 2021, DOI: 10.30501/jree.2021.275871.1194.

[16] B. Kurşun, "Thermal Performance Assessment Of Internal Longitudinal Fins With Sinusoidal Lateral Surfaces In Parabolic Trough Receiver Tubes," *Renew Energy*, vol. 140, pp. 816–827, Sep. 2019, DOI: 10.1016/j.renene.2019.03.106.

[17] H. L. Zhang, J. Baeyens, J. Degrève, and G. Cacères, "Concentrated Solar Power Plants: Review And Design Methodology," 2013, *Elsevier Ltd*. DOI: 10.1016/j.rser.2013.01.032.

[18] A. Yonanda, H. Naufal, Amrizal, M. Irsyad, Harmen, A. Riszal, J. B. Sinaga, and M. Haviz, "Performance evaluation of helix and spiral receiver geometries for a parabolic solar collector using CFD Analysis," 2025, Jurnal Polimesin Volume 23, No. 1, DOI: http://dx.doi.org/10.30811/jpl.v23i1.5709.

[19] Senthil Kumar Vishnu, and Ramalingam Senthil, "Experimental Performance Evaluation of a Solar Parabolic Dish Collector Using Spiral Flow Path Receiver," 2023, *Elsevier Ltd*. DOI: 10.1016/j.applthermaleng.2023.120979.

[20] Sumit Sharma, and Sandip K. Saha, "Development of Scaling Laws for Prototyping and Heat Loss Correlations for Upward Facing Cylindrical Helical Coil and Conical Spiral Coil Receivers," 2022, *Elsevier Ltd*. DOI: /10.1016/j.ijheatmasstransfer.2022.122773

[21] V. Thirunavukkarasu, and M. Cheralathan, "An Experimental Study On Energy And Exergy Performance of a Spiral Tube Receiver For Solar Parabolic Dish Concentrator," 2020, *Elsevier Ltd*. DOI: 10.1016/j.energy.2019.116635.

[22] Y. P. Chandra, S. K. Mohapatra, S. K. Mohapatra, and J. P. Kesari, “Concentrated Solar Thermal Energy : A Sustainable And Everlasting Form Of Renewable Energy,” 2012. [Online]. Available: https://www.researchgate.net/publication/305529506
[23] A. Z. Hafez, A. Soliman, K. A. El-Metwally, and I. M. Ismail, “Solar Parabolic Dish Stirling Engine System Design, Simulation, And Thermal Analysis,” *Energy Convers Manag*, vol. 126, pp. 60–75, Oct. 2016, DOI: 10.1016/j.enconman.2016.07.067.
[24] P. Dutta, “High Temperature Solar Receiver And Thermal Storage Systems,” *Appl Therm Eng*, vol. 124, pp. 624–632, 2017, DOI: 10.1016/j.applthermaleng.2017.06.028.
[25] R. Senthil and M. Cheralathan, “Enhancement Of The Thermal Energy Storage Capacity Of A Parabolic Dish Concentrated Solar Receiver Using Phase Change Materials,” *J Energy Storage*, vol. 25, Oct. 2019, DOI: 10.1016/j.est.2019.100841.
[26] Stasiun Meteorologi Radin Inten II. Buletin Stasiun Meteorologi Radin Inten II Lampung Selatan, edisi LXI. Lampung: BMKG; ISSN 2581-0790. Available from: https://www.lampung.bmkg.go.id
[27] J. P. Chiou, “The Effect Of Nonuniform Fluid Flow Distribution On The Thermal Performance Of Solar Collector,” 1982.
[28] J. Kim, J. S. Kim, and W. Stein, “Simplified Heat Loss Model For Central Tower Solar Receiver,” *Solar Energy*, vol. 116, pp. 314–322, Jun. 2015, DOI: 10.1016/j.solener.2015.02.022.
[29] K. B. Nguyen, S. H. Yoon, and J. H. Choi, “Effect Of Working-Fluid Filling Ratio And Cooling-Water Flow Rate On The Performance Of Solar Collector With Closed-Loop Oscillating Heat Pipe,” *Journal of Mechanical Science and Technology*, vol. 26, no. 1, pp. 251–258, Jan. 2012, DOI: 10.1007/s12206-011-1005-8.
[30] T. R. Jayawickrama, N. E. L. Haugen, M. U. Babler, M. A. Chishty, and K. Umeki, “The Effect Of Stefan Flow On Nusselt Number And Drag Coefficient Of Spherical Particles In Non-Isothermal Gas Flow,” *International Journal of Multiphase Flow*, vol. 140, Jul. 2021, DOI: 10.1016/j.ijmultiphaseflow.2021.103650.
[31] V. Thirunavukkarasu and M. Cheralathan, “An Experimental Study On Energy And Exergy Performance Of A Spiral Tube Receiver For Solar Parabolic Dish Concentrator,” Energy, vol. 192, Feb. 2020, DOI: 10.1016/j.energy.2019.116635.